obtained after immunoglobulin therapy in three of five patients with enterovirus-associated HLH (Table 1). Based on our observation and literature review, the accurate diagnosis of HLH in association with enterovirus, but not HSV or Epstein–Barr virus, may preclude the need for prompt immunochemotherapy.*LT*

Circulating IFN-γ levels are known to reflect HLH activity. IFN-γ-producing activated $CD8^+$ T cells is the pivotal player in the pathophysiology of FHL and EBV-HLH. In FHL, the defective mechanism of fratricide killing could fail to control the excessive activation of cytotoxic $CD8^+$ T cells. On the other hand, EBV-positive $CD8^+$ T cells are considered to be persistently activated in EBV-HLH patients. Recently, Xu et al. [9] reported that TLR9 stimulation precipitates macrophage activation and the development of HLH via IFN-γ-dependent, but not lymphocyte-dependent, pathways in which IL-10 plays a protective role. The present afebrile infant showed neither T-cell activation nor elevation of the serum IFN-γ and IL-10 levels at diagnosis despite exhibiting an overproduction of monokines. The first report on the cytokine profile of enterovirus-associated neonatal HLH might imply the other macrophage activation pathway. Neonates have a low capacity to produce IFN-γ. In contrast to our observation, a febrile neonate with HSV1-associated HLH showed high IFN-γ and IL-10 levels and attained successful remission [10]. IL-10 production regulates excessive inflammatory responses induced by IFN-γ [11]. It remains unclear whether the unique cytokine profile in the current patient represented the pathogen-specific or newborn-specific pathophysiology of HLH. However, the balanced IFN-γ/IL-10 production may predict a favorable course of virus-associated HLH. Further study of the cytokine profiles of neonatal HLH is needed to clarify the clinical expression of the disease and determine treatment strategies for affected patients.

Acknowledgments We thank Dr. Takahiro Yasumi (Department of Pediatrics, Kyoto University Hospital, Kyoto, Japan) and Prof. Eiichi Ishii (Department of Pediatrics, Ehime University Hospital, Toon, Japan) for their diagnostic support, and we appreciate the assistance of Dr. Brain Quinn for editing the English usage. This work was supported in part by a Grant-in-Aid for Scientific Research from the Ministry of Education, Culture, Sports, Science and Technology of Japan and by a grant from the Ministry of Health, Labour and Welfare of Japan.

Conflict of interest None.

References

1. Janka GE. Familial and acquired hemophagocytic lymphohistiocytosis. Annu Rev Med. 2012;3:233–46.
2. Risma K, Jordan MB. Hemophagocytic lymphohistiocytosis: updates and evolving concepts. Curr Opin Pediatr. 2012;24:9–15.
3. Henter JI, Horne A, Aricó M, Egeler RM, Filipovich AH, Imashuku S, et al. HLH-2004: diagnostic and therapeutic guidelines for hemophagocytic lymphohistiocytosis. Pediatr Blood Cancer. 2007;48:124–31.
4. Barre V, Marret S, Mendel I, Lesesve JF, Fessard CI. Enterovirus-associated haemophagocytic syndrome in a neonate. Acta Paediatr. 1998;87:469–71.
5. Lindamood KE, Fleck P, Narla A, Vergilio JA, Degar BA, Baldwin M, et al. Neonatal enteroviral sepsis/meningoencephalitis and hemophagocytic lymphohistiocytosis: diagnostic challenges. Am J Perinatol. 2011;28:337–46.
6. Suzuki N, Morimoto A, Ohga S, Kudo K, Ishida Y, Ishii E. Characteristics of hemophagocytic lymphohistiocytosis in neonates: a nationwide survey in Japan. J Pediatr. 2009;155:235–8.
7. Khetsuriani N, Lamonte-Fowlkes A, Oberst S, Pallansch MA. Enterovirus surveillance–United States, 1970–2005. MMWR Surveill Summ. 2006;55:1–20.
8. Schwab I, Nimmerjahn F. Intravenous immunoglobulin therapy: how does IgG modulate the immune system? Nat Rev. 2013;13:176–89.
9. Xu XJ, Tang YM, Song H, Yang SL, Xu WQ, Zhao N, et al. Diagnostic accuracy of a specific cytokine pattern in hemophagocytic lymphohistiocytosis in children. J Pediatr. 2012;160:984–90.
10. Yamada K, Yamamoto Y, Uchiyama A, Ito R, Aoki Y, Uchida Y, et al. Successful treatment of neonatal herpes simplex-type 1 infection complicated by hemophagocytic lymphohistiocytosis and acute liver failure. Tohoku J Exp Med. 2008;214:1–5.
11. Behrens EM, Canna SW, Slade K, Rao S, Kreiger PA, Paessler M, et al. Repeated TLR9 stimulation results in macrophage activation syndrome-like disease in mice. J Clin Invest. 2011;121:2264–77.

Higuchi et al. Pediatric Rheumatology 2013, 11:41
http://www.ped-rheum.com/content/11/1/41

PEDIATRIC RHEUMATOLOGY

CASE REPORT Open Access

The identification of a novel splicing mutation in *C1qB* in a Japanese family with C1q deficiency: a case report

Yousuke Higuchi[1], Junya Shimizu[1*], Michiyo Hatanaka[2], Etsuko Kitano[2], Hajime Kitamura[2], Hidetoshi Takada[3], Masataka Ishimura[3], Toshiro Hara[3], Osamu Ohara[4], Kenji Asagoe[5] and Toshihide Kubo[1]

Abstract

C1q deficiency is a rare disease that is associated with a high probability of developing systemic lupus erythematosus. We report a 4-year-old Japanese girl who presented with fever, facial erythema, joint pain, and oral ulceration. Complement deficiencies were suspected because of her persistent hypocomplementemia and normal levels of the complement proteins C3 and C4. We identified a novel homozygous splicing mutation in the *C1qB* gene, c.187 + 1G > T, which is the first mutation to be confirmed in a Japanese individual. Because treatment with steroids and immunosuppressive drugs was not effective, we commenced use of fresh frozen plasma to provide C1q supplements. Currently, the patient remains almost asymptomatic, and we are attempting to control the drug dosage and administration intervals of fresh frozen plasma.

Keywords: C1q deficiency, Systemic lupus erythematosus, Hypocomplementemia, Novel mutation, Fresh frozen plasma

Background

The complement system involves a group of proteins that function as part of the immune system. Three complement pathways make up the complement system, the classical, alternative, and lectin pathways. The C1q protein is the first component of the classical pathway and is composed of the C1qA chain, C1qB chain, and C1qC chain, which are encoded by *C1qA*, *C1qB*, and *C1qC* genes, respectively [1].

C1q deficiency is a rare disease that is associated with a high probability of developing systemic lupus erythematosus (SLE) [2,3]. It is also complicated by cutaneous disease, glomerulonephritis, central nerve system lupus, and recurrent bacterial infection at an early age [2,4]. A deficiency of other complement components such as C1r, C1s, C2, and C4 is also involved in SLE, with C1q deficiency being the strongest single risk factor for SLE development [5]. The first C1q deficiency-causing mutation was reported by McAdam et al. in 1988 [6]. Today, 14 mutations have been identified, all of which are nonsense or missense mutations [7-9]. Although immunosuppressive therapy is administered to C1q deficiency patients, there is currently no curative therapy.

We report herein a girl with C1q deficiency, and the identification of a novel splice site mutation in the *C1qB* gene, which is the first confirmed genetic mutation in a Japanese individual with C1q deficiency.

Case presentation

A 4-year-old Japanese girl was referred to our hospital with a three month history of fever, facial erythema, joint pain, and oral ulceration. She had been diagnosed with discoid lupus erythematosus following a skin biopsy at another hospital. Her symptoms were alleviated transiently after the oral administration of prednisolone; however, they relapsed after cessation of treatment. She had no past history of recurrent infections or fevers of unknown origin. Her parents are not consanguineous,

* Correspondence: junshimi@okayama3.hosp.go.jp
[1]Department of Pediatrics, National Hospital Organization Okayama Medical Center, 1711-1 Tamasu, Kita-ku, Okayama 701-1192, Japan
Full list of author information is available at the end of the article

and all other family members, including parents and two brothers, were healthy and had not complained of SLE-like symptoms at that time.

At the first visit to our department, physical examinations revealed low grade fever, scarring facial erythema, oral ulceration, and a chilblain-like rash on the extremities of her limbs (Figure 1). Breath sounds were clear and unlabored. Cardiac examination revealed no murmurs, rubs, or gallops. The abdomen was soft, nontender, and nondistended. Neurological examinations of the cranial nerve, motor strength and coordination, reflexes, gait and sensation were normal. Blood and urine tests for rheumatic fever and other febrile illness revealed elevated inflammatory markers (erythrocyte sedimentation rate (ESR) 65 mm/60 min, C-reactive protein (CRP) 1.32 mg/dl), although blood cell count, electrolytes, blood urea nitrogen, creatinine, liver function, and urinary tests were all normal (Table 1). Total complement activity (CH50) was not detectable but an immunoturbidimetric assay revealed that C3 and C4 levels were within the normal range. Speckled antinuclear antibody and rheumatoid factor were positive, and anti-double stranded DNA IgG antibody levels were negative. A chest computed tomography (CT), echocardiography, magnetic resonance imaging of the brain, and renal biopsy specimen were normal.

Figure 1 Lupus erythematosus malar skin rash and rash on the hand and foot of our patient.

Initially, the patient had been diagnosed with SLE and had received prednisolone and mizoribine treatment. Although symptoms ameliorated immediately, CH50 remained consistently negative during a period of six months, whereas C3 and C4 were within the normal range. Antinuclear antibody and rheumatoid factor levels gradually elevated, but anti-double stranded DNA IgG antibody levels were still negative. From the above discrepancy between symptoms and laboratory data changes, we suspected complement deficiency so investigated her complement system in detail. Serum C1q levels measured at SRL Inc. (Tokyo, Japan) by nephelometry were 2.8 mg/dl (normal range: 8.8–15.3 mg/dl). Further analysis of the complement systems revealed that whole alternative complement pathway activity (ACH50) and C4 and C2 activities were within the normal range, whereas C1 activity was very low (Table 2) [10-13]. The addition of purified human C1 subcomponent enabled CH50 to be restored to a normal range only when C1q was added, but neither C1r nor C1s was effective (Table 3). For this reason, we strongly suspected a C1q deficiency.

Genomic DNA was extracted from EDTA-blood cells using standard procedures. PCR primers were designed to amplify all exons and exon-intron boundaries of *C1qA*, *C1qB* and *C1qC* genes. Table 4 shows the primer sets and sequencing performed with the BigDye terminator v3.1 Cycle Sequencing Kit. Sequence analysis revealed a novel homozygous splice site mutation in *C1qB*, c.187 + 1G > T (Figure 2), but no other mutations. Reverse transcriptase-polymerase chain reaction amplification of *C1qB* demonstrated the presence of an abnormal single band on gel electrophoresis caused by a splicing error of intron 2/intron 3 (Figure 3). Combined with the complement assay, this DNA sequencing result enabled the molecular diagnosis of C1q deficiency to be confirmed. Mutation analysis and CH50 measurements of family members demonstrated that the patient's parents and one sibling were heterozygous for c.187 + 1G > T with normal CH50 levels. The second sibling (0 years old) with undetectable CH50 levels was also homozygous for the mutation (Figure 4).

After about one year from the first visit, the patient experienced a recurrent fever every few days with no

Table 1 Laboratory findings on first visit of patient

Blood test	Result	Normal range	Blood test	Result	Normal range
WBC	6600/μl	4500–15500	CRP	1.32 mg/dl	<0.1
Seg	5600/μl	1500–8500	ESR 60 min	65 mm/60 min	0–15
Ly	660/μl	1200–8000			
RBC	379×10^4/μl	390–490	CH50	<12.0 CH50/ml	22–40
Hb	10.7 g/dl	11.4–14.2	C3	122 mg/dl	71–159
Ht	30.5%	34–40	C4	45 mg/dl	13–30
Plt	15.2×10^4/μl	14.0–45.0	RF	31 IU/ml	<40
AST	31 IU/l	18–63	ANA(speckled)	1:320	<1:40
ALT	21 IU/l	20–50	Anti-dsDNA IGG	<10 IU/ml	<10
LDH	297 IU/l	142–297	Anti-Sm	1:2	<1:2
Na	141 mEq/l	134–143	Anti-RNP	1:16	<1:2
K	3.3 mEq/l	3.4–4.9	Anti-Ro	(–)	(–)
Cl	104 mEq/l	98–107	Anti-La	(–)	(–)
Ca	9.0 mg/dl	8.8–10.3			
TP	6.3 g/dl	5.6–7.7	Urinalysis		
Alb	3.8 g/dl	3.1–4.8	U-protein	(–)	(–)
BUN	6 mg/dl	5–27	U-glucose	(–)	(–)
Cre	0.40 mg/dl	0.30–0.90	U-occult blood	(–)	(–)

sign of infection. Despite increasing the doses of prednisolone (15 mg/day) and mizoribine (300 mg/every other day), fever and erythematosus rash were aggravated and the ESR elevated to 68 mm/60 min, which is the index that most reflects her condition. We carried out intravenous methylprednisolone pulse therapy, but the effect was only temporary. Accordingly, we initiated fresh frozen plasma (FFP) transfusion for supplementation of C1q. Immediately after transfusion of FFP (10 ml/kg), her CH50 levels recovered to within the normal range but became undetectable 24 h later (Table 5). Nevertheless, she remained afebrile and her rash improved slowly, while ESR declined to 37 mm/60 min following once weekly administration of FFP (10 ml/kg). We are currently attempting to slowly reduce the prednisolone dosage and the frequency of FFP.

Conclusions

We report a girl diagnosed with SLE because of C1q deficiency caused by a novel homozygous splice site mutation in *C1qB*. C1q deficiency is a rare autosomal recessively inherited disease, with only 41 patients from 23 families reported in 1998 [2]. More recently, C1q deficiency has been confirmed in 64 cases within 38 families, 88% of which present with SLE or SLE-like disease [7].

Table 2 Analysis of complement system activity

Hemolytic activity	NHS	Patient serum	Reference value
CH50 (U/ml)	125	0	90–160
(NHS %)	100%	0%	
ACH50 (U/ml)	18.5	18.9	
(NHS %)	100%	102%	70–130%
C1 activity (U/ml)	1450	100	
(NHS %)	100%	7%	70–130%
C2 activity (U/ml)	400	360	
(NHS %)	100%	90%	70–130%
C4 activity (U/ml)	2000	1600	
(NHS %)	100%	80%	70–130%

NHS normal human serum, *ACH50* alternative complement pathway activity.

Table 3 Addition of purified human C1 subcomponent

Hemolytic activity	NHS
CH50 (U/ml)	125
(NHS %)	100%
Patient serum + C1q (U/ml)	140
(NHS %)	112%
Patient serum + C1r (U/ml)	0
(NHS %)	0%
Patient serum + C1s (U/ml)	0
(NHS %)	0%
Patient serum + activated C1s (U/ml)	0
(NHS %)	0%

NHS normal human serum.

Table 4 List of primers used in this work

Primer name	Gene	Exon	F/R	Primer sequence (5'-3')	Tm (°C)	Annealing Tm (°C)
C1QA-02-F	C1qA	02	F	TTGTGTGCATGGGACTCAAG	56	60
C1QA-02-R	C1qA	02	R	GGCCAAGTCAGGCCAAG	58	
C1QA-03a-F	C1qA	03a	F	TCCCTGAGGACCAGTAGGC	60	60
C1QA-03a-R	C1qA	03a	R	GGACAGGCAGATTTCCCAC	58	
C1QA-03b-F	C1qA	03b	F	TCATCTTCGACACGGTCATC	56	60
C1QA-03b-R	C1qA	03b	R	ATTTTACAGGCGGAGCATGG	56	
C1QB-02-F	C1qB	02	F	GGATGCAGATGGAGGGATAG	58	60
C1QB-02-R	C1qB	02	R	AGGCAACTGTGACTTGGGAG	58	
C1QB-03a-F	C1qB	03a	F	GCAGGCCTCCTTCTTTTGG	58	60
C1QB-03a-R	C1qB	03a	R	TCACGCACAGGTTCCCTC	58	
C1QB-03b-F	C1qB	03b	F	CAGACCATCCGCTTCGAC	58	60
C1QB-03b-R	C1qB	03b	R	GGGGTAGAGTGAGCGTTGC	60	
C1QC-02-F	C1qC	02	F	ATCCATGGTGAGGCTCCTG	58	60
C1QC-02-R	C1qC	02	R	CCCAGACAGACACTCTGATCC	60	
C1QC-03a-F	C1qC	03a	F	GTTCCCTGGAAGACACCCTC	60	60
C1QC-03a-R	C1qC	03a	R	TATGCGACGCGTGGTAGAC	58	
C1QC-03b-F	C1qC	03b	F	AGCCTGATCAGATTCAACGC	56	60
C1QC-03b-R	C1qC	03b	R	TGGCCAGTAAGGTGGGTCC	60	

F forward, *R* reverse, *Tm* temperature.

There are three hypotheses regarding the relationship between C1q deficiency and SLE or SLE-like disease. The first is that C1q deficiency causes autoimmunity by impairing the clearance of apoptotic cells [2], while in the second the absence of C1q affects the negative selection of autoreactive B cells [14]. The third is that the lack of C1q leads to increased interferon-α production and the defective regulation of dendritic cells [15]. It has also been reported that C1q activates canonical Wnt signaling, which regulates T cell development and dendritic cell maturation [16-18]. The suppression of Wnt signaling in association with C1q deficiency may result in the inadequate activation of lymphocytes.

The majority of C1q deficiency patients are European or Middle Eastern, with only four cases reported to

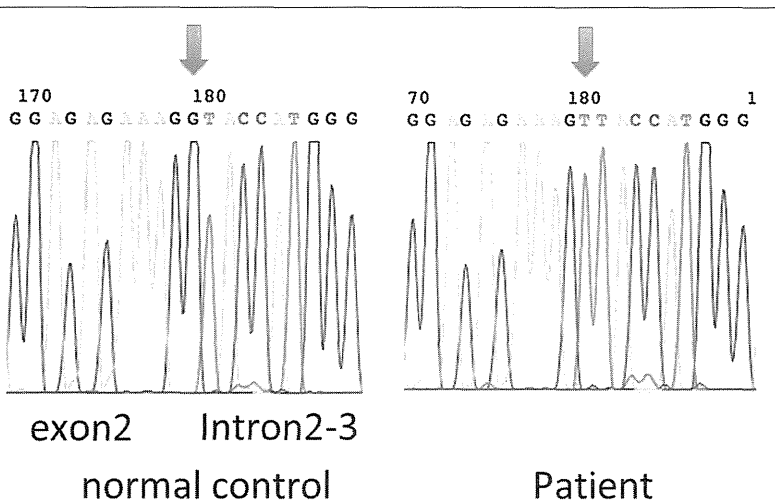

Figure 2 Sequence analysis of the *C1qB* gene. A homozygous mutation was identified at the consensus splicing donor site in intron 2–3 caused by a G-to-T transversion (c.187 + 1G > T).

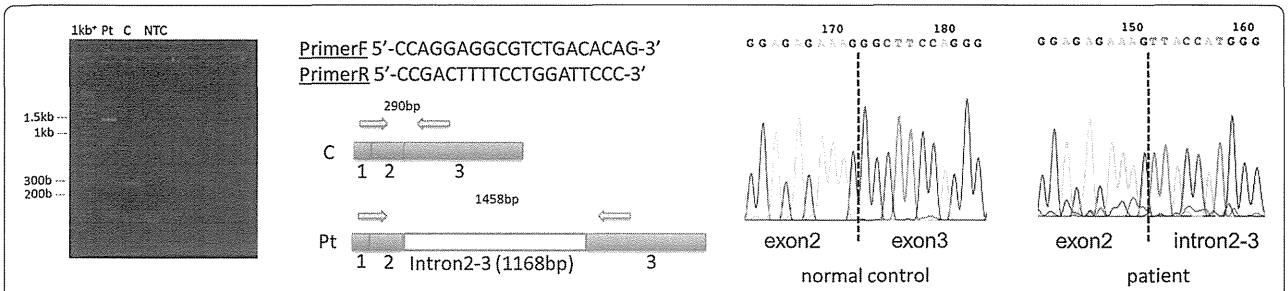

Figure 3 Reverse transcriptase-polymerase chain reaction analysis of *C1qB* mRNA. A single band observed at 1458 bp was caused by a splicing error of intron 2–3. 1 kb+, 1,000 bp DNA-ladder marker; Pt., patient; C., normal control; NTC, no template control.

date in Japan, none of which were confirmed by genetic analysis [7,19-22]. Al-Mayouf et al. reported that C1q deficiency patients tend to develop SLE in less than five years [4]. Our patient also developed SLE at the age of four, with persistent hypocomplementemia and normal C3 and C4 levels. We believe that the possibility of C1q deficiency should therefore always be considered in such cases. To our knowledge, 14 different C1q deficiency-causing mutations have been identified to date, most in European and Middle Eastern patients, with one in an African-American ancestry [7-9]. All are missense or nonsense mutations, so the present mutation is the first report of a splicing error associated with the disorder.

Previously reported complications of C1q deficiency include glomerulonephritis in 30%, central nervous system involvement in 19%, and bacterial infections in 41% of patients [7]. Moreover, symptoms present with varying degrees of severity, even in the same family [23]. It is possible that environmental factors such as exposure to ultraviolet radiation or a history of infection may affect the epigenetic regulation of developing SLE-like syndrome. In our case, the patient may develop complications later in life, and her homozygous sibling may also develop SLE. It is therefore important to carefully follow up our patients to prevent the onset of glomerulonephritis and central nervous system involvements.

At present, no specific therapy is available for C1q deficiency, so steroids and immunosuppressive agents such as hydroxychloroquine (not currently available in Japan) are used as treatments. Bone marrow transplantation is a potential cure, but it has not yet been performed in humans [24,25]. Some reports show that the infusion of FFP restores C1q levels, temporarily complements hemolytic activity, and suppresses SLE symptoms for a long period [8,24]. It is therefore a valid therapy for C1q deficiency patients. However, the long-term administration of FFP increases the risk of infection and the possibility of side effects caused by the development of anti-C1q antibodies [26]. In the light of such risks, alternative treatment strategies should be considered for this intractable disease.

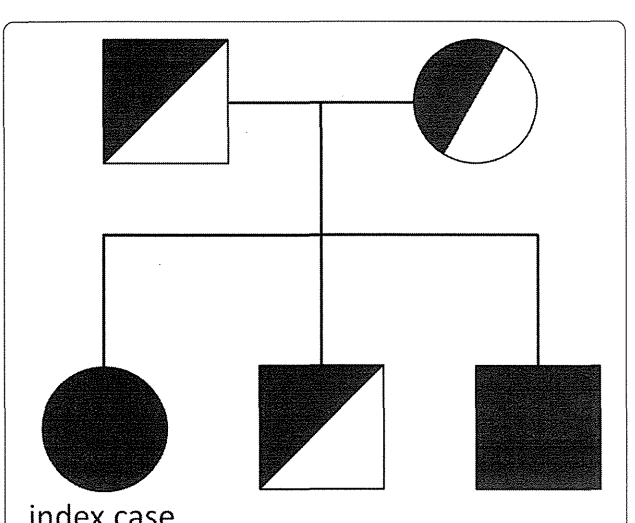

Figure 4 Pedigree showing the heterozygosity of the patient's parents and older brother, and the homozygosity of her younger brother, for c.187 + 1G > T.

Consent

Written informed consent was obtained from the patient for publication of this Case Report and any accompanying images. A copy of the written consent is available for review from the Editor-in-Chief of this journal.

Table 5 Measurement of CH50 following transfusion of FFP in the patient

Time (hr)	0	3 (end of transfusion)	9	24
CH50 (U/ml)	<12.0	25.5	24.6	<12.0

Abbreviations
SLE: Systemic lupus erythematosus; ESR: Erythrocyte sedimentation rate; CRP: C-reactive protein; CH50: Total complement activity; CT: Computed tomography; FFP: Fresh frozen plasma.

Competing interests
The authors have nothing to disclose.

Authors' contributions
YH drafted the manuscript, and participated in treatment. JS, KA, and TK carried out the clinical treatment and helped draft the manuscript. MH, EK, and HK analyzed the complement systems and interpreted the data. HT, MI, TH, and OO sequenced the *C1q* genes and performed reverse transcriptase-polymerase chain reaction analysis of *C1qB* mRNA. All authors read and approved the final manuscript.

Acknowledgement
We thank Edanz (http://www.edanzediting.co.jp) for English writing assistance.

Author details
[1]Department of Pediatrics, National Hospital Organization Okayama Medical Center, 1711-1 Tamasu, Kita-ku, Okayama 701-1192, Japan. [2]Department of Medical Technology Faculty of Health Sciences, Kobe Tokiwa University, 2-6-2 Ohtanicho, Nagata-ku, Kobe 653-0838, Japan. [3]Department of Pediatrics, Graduate School of Medical Sciences, Kyushu University, 3-1-1 Maidashi, Higasi-ku, Fukuoka 812-8582, Japan. [4]Department of Human Genome Technology, Kazusa DNA Research Institute, 2-6-7 Kazusakamatari, Chiba 292-0818, Japan. [5]Department of Dermatology, National Hospital Organization Okayama Medical Center, 1711-1 Tamasu, Kita-ku, Okayama 701-1192, Japan.

Received: 13 August 2013 Accepted: 25 October 2013
Published: 28 October 2013

References

1. Kishore U, Reid KB: **C1q: structure, function, and receptors.** *Immunopharmacology* 2000, **49**:159–170.
2. Walport MJ, Davies KA, Botto M: **C1q and systemic lupus erythematosus.** *Immunobiology* 1998, **199**:265–285.
3. Walport MJ: **Complement and systemic lupus erythematosus.** *Arthritis Res* 2002, **4**(Suppl 3):279–293.
4. Al-Mayouf SM, Abanomi H, Eldali A: **Impact of C1q deficiency on the severity and outcome of childhood systemic lupus erythematosus.** *Int J Rheum Dis* 2011, **14**:81–85.
5. Pickering MC, Botto M, Taylor PR, Lachmann PJ, Walport MJ: **Systemic lupus erythematosus, complement deficiency, and apoptosis.** *Adv Immunol* 2000, **76**:227–324.
6. McAdam RA, Goundis D, Reid KB: **A homozygous point mutation results in a stop codon in the C1q B-chain of a C1q-deficient individual.** *Immunogenetics* 1988, **27**:259–264.
7. Schejbel L, Skattum L, Hagelberg S, Åhlin A, Schiller B, Berg S, Genel F, Truedsson L, Garred P: **Molecular basis of hereditary C1q deficiency–revisited: identification of several novel disease-causing mutations.** *Genes Immun* 2011, **12**:626–634.
8. Namjou B, Keddache M, Fletcher D, Dillon S, Kottyan L, Wiley G, Gaffney PM, Wakeland BE, Liang C, Wakeland EK, Scofield RH, Kaufman K, Harley JB: **Identification of novel coding mutation in C1qA gene in an African-American pedigree with lupus and C1q deficiency.** *Lupus* 2012, **21**:1113–1118.
9. Topaloglu R, Taskiran EZ, Tan C, Erman B, Ozaltin F, Sanal O: **C1q deficiency: identification of a novel missense mutation and treatment with fresh frozen plasma.** *Clin Rheumatol* 2012, **31**:1123–1126.
10. Kobayashi E, Kitano E, Kitamura H: **A novel assay for serum complement activity: C42 generation assay.** *Int Arch Allergy Immunol* 1999, **120**:71–77.
11. Kitamura H, Nishimukai H, Sano Y, Nagaki K: **Study on C3-like factor in the serum of a C3-deficient subject.** *Immunology* 1984, **51**:239–245.
12. Kitano E, Kitamura H: **Dual effects of TNF on synthesis of complement components by a gastric cancer-derived cell line, KATO-III.** *Int Arch Allergy Immunol* 1999, **119**:54–59.
13. Whaley K, North J: **Haemolytic assays for whole complement activity and individual components.** In *Complement: A Practical Approach.* Edited by Dodds AW, Sim RB. Oxford: IRL Press; 1997:19–47.
14. Yurasov S, Wardemann H, Hammersen J, Tsuiji M, Meffre E, Pascual V, Nussenzweig MC: **Defective B cell tolerance checkpoints in systemic lupus erythematosus.** *J Exp Med* 2005, **201**:703–711.
15. Santer DM, Hall BE, George TC, Tangsombatvisit S, Liu CL, Arkwright PD, Elkon KB: **C1q deficiency leads to the defective suppression of IFN-alpha in response to nucleoprotein containing immune complexes.** *J Immunol* 2010, **185**:4738–4749.
16. Naito AT, Sumida T, Nomura S, Liu ML, Higo T, Nakagawa A, Okada K, Sakai T, Hashimoto A, Hara Y, Shimizu I, Zhu W, Toko H, Katada A, Akazawa H, Oka T, Lee JK, Minamino T, Nagai T, Walsh K, Kikuchi A, Matsumoto M, Botto M, Shiojima I, Komuro I: **Complement C1q activates canonical Wnt signaling and promotes aging-related phenotypes.** *Cell* 2012, **149**:1298–1313.
17. Manicassamy S, Reizis B, Ravindran R, Nakaya H, Salazar-Gonzalez RM, Wang YC, Pulendran B: **Activation of beta-catenin in dendritic cells regulates immunity versus tolerance in the intestine.** *Science* 2010, **329**:849–853.
18. Xu Y, Banerjee D, Huelsken J, Birchmeier W, Sen JM: **Deletion of beta-catenin impairs T cell development.** *Nat Immunol* 2003, **4**:1177–1182.
19. Nishino H, Shibuya K, Nishida Y, Mushimoto M: **Lupus erythematosus-like syndrome with selective complete deficiency of C1q.** *Ann Intern Med* 1981, **95**:322–324.
20. Uenaka A, Akimoto T, Aoki T, Tsuyuguchi I, Nagaki K: **A complete selective C1q deficiency in a patient with discoid lupus erythematosus (DLE).** *Clin Exp Immunol* 1982, **48**:353–358.
21. Orihara T, Tsuchiya K, Yamasaki S, Furuya T: **Selective C1q deficiency in a patient with systemic lupus erythematosus.** *Br J Dermatol* 1987, **117**:247–254.
22. Hayakawa J, Migita M, Ueda T, Itoh Y, Fukunaga Y: **Infantile case of early manifestation of SLE-like symptoms in complete C1q deficiency.** *J Nippon Med Sch* 2011, **78**:322–328.
23. Vassallo G, Newton RW, Chieng SE, Haeney MR, Shabani A, Arkwright PD: **Clinical variability and characteristic autoantibody profile in primary C1q complement deficiency.** *Rheumatology (Oxford)* 2007, **46**:1612–1614.
24. Mehta P, Norsworthy PJ, Hall AE, Kelly SJ, Walport MJ, Botto M, Pickering MC: **SLE with C1q deficiency treated with fresh frozen plasma: a 10-year experience.** *Rheumatology (Oxford)* 2010, **49**:823–824.
25. Cortes-Hernandez J, Fossati-Jimack L, Petry F, Loos M, Izui S, Walport MJ, Cook HT, Botto M: **Restoration of C1q levels by bone marrow transplantation attenuates autoimmune disease associated with C1q deficiency in mice.** *Eur J Immunol* 2004, **34**:3713–3722.
26. Bowness P, Davies KA, Norsworthy PJ, Athanassiou P, Taylor-wiedeman J, Borysiewicz LK, Meyer PAR, Walport MJ: **Hereditary C1q deficiency and systemic lupus erythematosus.** *QJM* 1994, **87**:455–464.

doi:10.1186/1546-0096-11-41
Cite this article as: Higuchi *et al.*: The identification of a novel splicing mutation in *C1qB* in a Japanese family with C1q deficiency: a case report. *Pediatric Rheumatology* 2013 **11**:41.

J Infect Chemother (2013) 19:757–760
DOI 10.1007/s10156-012-0493-5

CASE REPORT

Two cases of partial dominant interferon-γ receptor 1 deficiency that presented with different clinical courses of bacille Calmette–Guérin multiple osteomyelitis

Kaoru Obinata · Tsubasa Lee · Takahiro Niizuma · Keiji Kinoshita · Toshiaki Shimizu · Takayuki Hoshina · Yuka Sasaki · Toshiro Hara

Received: 2 May 2012 / Accepted: 21 September 2012 / Published online: 11 October 2012

Abstract We experienced two cases of unrelated Japanese children with bacille Calmette–Guérin (BCG) multiple osteomyelitis with partial interferon (IFN)-γ receptor 1 (IFNGR1) deficiency. Heterozygous small deletions with frame shift (811 del4 and 818 del4) were detected, which were consistent with the diagnosis of partial dominant IFNGR1 deficiency. Case 1: a 2-year-old boy visited us because of limb and neck pain. He had been vaccinated with BCG at 17 months of age. Multiple destructive lesions were observed in the skull, ribs, femur, and vertebral bones. *Mycobacterium bovis* (BCG Tokyo 172 strain by RFLP technique) was detected in the bone specimen. The BCG multiple osteomyelitis was treated successfully without recurrence. Case 2: an 18-month-old girl developed multiple osteomyelitis 9 months after BCG inoculation. Radiologic images showed multiple osteolytic lesions in the skull, ribs, femur, and vertebrae. *M. bovis* (BCG Tokyo 172 strain) was detected in the cultures from a bone biopsy. Her clinical course showed recurrent osteomyelitis and lymphadenitis with no pulmonary involvement. The effects of high-dose antimycobacterial drugs and IFN-γ administration were transient, and complete remission has since been achieved by combination antimycobacterial therapy, including levofloxacin. Partial dominant IFNGR1 deficiency is a rare disorder, but it should be considered when a patient presents with multiple osteomyelitis after BCG vaccination. The cases that are resistant to conventional regimens require additional second-line antituberculous drugs, such as levofloxacin.

Keywords Interferon-γ receptor 1 deficiency · Multiple osteomyelitis · Bacille Calmette–Guérin · Mycobacterial infection · Levofloxacin

Introduction

Interleukin-12 (IL-12)- and IFN-γ (IFNG)-mediated immunity plays an important role in host defense against intracellular pathogens [1]. Mendelian susceptibility to mycobacterial disease (MSMD) is a rare disorder and sometimes lethal disease that occurs in response to poorly virulent mycobacteria, such as bacille Calmette–Guérin (BCG) and environmental nontuberculous mycobacteria (NTM). In patients with MSMD, different types of mutations in six genes—IFNGR1, IFNGR2, IL12RB1, IL12B, STAT-1, and NEMO—have been revealed [2].

Sasaki et al. [3] previously reported a partial IFNGR1 mutation in three Japanese children with BCG osteomyelitis and in the father of one of the patients. We have followed the two unrelated cases over 10 years since their onset in the same department (Koshigaya Municipal Hospital). Based on our longitudinal experience, we intend to provide important clinical information for the diagnosis and treatment of IFN-γR1 deficiency in Japan.

K. Obinata · T. Lee · T. Niizuma · K. Kinoshita
Department of Pediatrics, Koshigaya Municipal Hospital, Saitama, Japan

K. Obinata (✉)
Department of Pediatrics, Juntendo University Urayasu Hospital, 2-1-1 Tomioka, Urayasu, Chiba 279-0021, Japan
e-mail: obinata@juntendo-urayasu.jp

T. Shimizu
Department of Pediatrics, Faculty of Juntendo University, Tokyo, Japan

T. Hoshina · Y. Sasaki · T. Hara
Department of Pediatrics, Graduate School of Medical Science, Kyushu University, Fukuoka, Japan

Case report

Case 1

A Japanese boy became spontaneously positive to a tuberculin purified protein derivative (PPD) skin test at the age of 11 months. There was no family history of tuberculosis. A chest X-ray film showed no abnormal findings. The PPD skin test turned negative after 6 months of prophylactic treatment with isoniazid (INH). He was inoculated with BCG (Tokyo 172 strain) by the multiple puncture technique at the age of 17 months. Nine months later (at 26 months of age), he started to limp and could not move his neck. He visited Koshigaya Municipal Hospital, and multiple osteolytic lesions were observed on his skull, vertebrae (cervical and lumbar), ribs, and femur by X-ray, bone scintigram, and magnetic resonance (MR) imaging. *Mycobacterium* was detected in the bone biopsy. *Mycobacterium bovis* was identified as the BCG Tokyo 172 strain by restriction fragment length polymorphism (RFLP). The BCG osteomyelitis was treated successfully with antimycobacterial therapy with isoniazid (INH), rifampicin (RFP), and streptomycin (SM) for 1.5 years without recurrence. He is now 17 years old and has not had a mycobacterial infection since the treatment.

Case 2 (Fig. 1)

An 18-month-old girl (13 years old at present) developed left axillary lymphadenitis 2 months after BCG inoculation at the age of 8 months. Multiple skin eruptions and abscesses appeared 9 months after the vaccination. At the BCG inoculation site, there were signs of hypertrophic scar and keloid. Granuloma was also observed below the inoculation site. X-ray, skeletal scintigram, and MR imaging showed multiple osteolytic lesions in the skull, ribs, femur, and vertebrae. A bone biopsy specimen of the femur revealed granulomatous inflammation without central necrosis. *M. bovis* (BCG Tokyo 172 strain) was detected in cultures from the bone biopsy by RFLP. She was treated with INH, RFP, and SM, and showed slow improvement. Eighteen months after her initial presentation, she started to develop recurrent osteomyelitis. Additional administration of ethambutol (EB) and IFN-γ was effective but the effect was temporary. She exhibited osteomyelitis soon after discontinuation of EB and RFP. High-dose INH and EB, with the addition of clarithromycin (CAM) and IFN-γ, proved effective. Her osteomyelitis appeared to have subsided. However, later, at the age of 11 years, she experienced a third relapse of the osteomyelitis. Antimycobacterial therapy was started again, but lymphadenitis also developed on her right supraclavicle. The findings from the swollen lymph nodes were nonspecific. Additional administration of high-dose IFN-γ was partially effective against the osteomyelitis and the lymphadenitis. As the cervical lymphadenopathy appeared again, the CAM was changed to levofloxacin (LVFX). A three-drug regimen of INH, RFP, and LVFX for a period of 9 months was successful in achieving remission.

The clinical features of these two unrelated Japanese children with BCG multiple osteomyelitis are summarized in Table 1. Two-color flow cytometric analysis was performed [3] and showed significantly higher levels of IFNGR1 expression on monocytes in both cases. IL-12 and IFN-γ production was normal. Genomic DNA was obtained from peripheral blood mononuclear cells. cDNA sequences were analyzed by polymerase chain reaction. Heterozygous small deletions with frame shift (case 1, 811 del4; case 2,

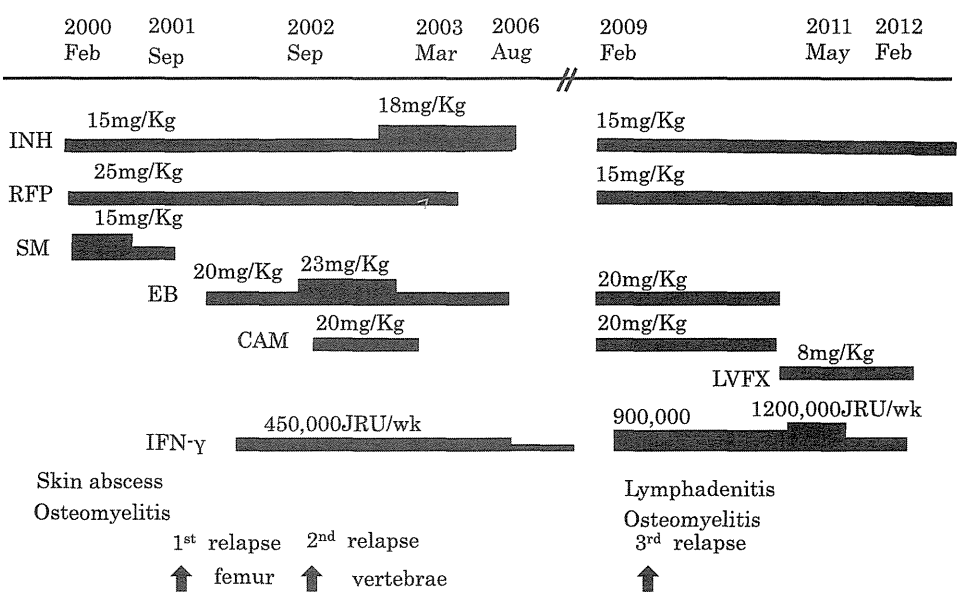

Fig. 1 Recurrent osteomyelitis and lymphadenitis in case 2. *INH* isoniazid, *RFP* rifampicin, *SM* streptomycin, *EB* ethambutol, *CAM* clarithromycin

Table 1 Immunological data at the onset of patients with bacille Calmette–Guérin (BCG) osteomyelitis

Case	1 (17 years/M)	2 (13 years/F)
BCG given at	1 year 5 months	8 months
Age at onset	2 years 2 months	1 year 5 months
Type	Multiple	Multiple, recurrent
Histology	Inflammation	Granuloma
Other organs	None	Skin, lymph node
WBCs/μl	5,300	29,600
Lymphocytes/μl	3,657	7,400
IgG, mg/dl	1,370	1,430
IgA, mg/dl	188	104
IgM, mg/dl	602	181
CD3 cells, %	40.7	56.6
CD4:CD8	3	3
CD19 cells, %	10.4	26.4
PHA response	Normal	Normal
Cytokine production IL-12/INF-γ	Normal	Normal

818 del4) were detected, which were consistent with the diagnosis of partial dominant IFNGR1 deficiency (data not shown). Sequence analysis of six coding regions was performed and showed that none of the family members of the patients had any mutations. Furthermore, neither sets of parents were consanguineous. Thus, de novo mutation had occurred in both cases 1 and 2.

Discussion

Bacille Calmette–Guérin vaccines are safe in immunocompetent hosts, and Japanese BCG substrain Tokyo 172 is the safest BCG in the world [4]. Complications of BCG vaccination can be severe and life threatening in infants with immunodeficiency. Systemic adverse reactions to BCG vaccine, including osteomyelitis and disseminated BCG infection, are rare. Toida and Nakata [5] reviewed severe adverse reactions to BCG from 1951 to 2004 in Japan and identified 39 cases (incidence rate, 0.0182 cases per 100,000 vaccinations). Thirteen cases exhibited primary immunodeficiency; 5 of these exhibited chronic granulomatous diseases, 4 exhibited severe combined immunodeficiency, and 4 exhibited IFNGR1 deficiency. Unidentified defects in cellular immunity were observed in 6 cases. The 6 fatal cases had cellular immunodeficiencies. Bone and joint involvement was observed in 27 cases, 15 cases with multiple lesions and 12 cases with single site lesions.

Hoshina et al. [6] analyzed the clinical characteristics and the genetic background of 46 patients with MSMD in Japan from 1999 to 2009, and found that 6 had mutations in the IFN-γR1 gene. All the cases of IFN-γR1 deficiency exhibited multiple osteomyelitis, and disseminated mycobacterial infection recurred in 5 patients. All the patients exhibited the partial dominant type, and 4 of them had 818 del4. Two of the patients were from the same family, and therefore autosomal dominant inheritance was suspected. The 4 others were considered to have occurred spontaneously. In Taiwan, 3 patients from two unrelated families were identified with a hotspot IFNGR1 deletion mutation (818 del4) and exhibited chronic granulomatous disease-like features, presenting as cutaneous granuloma and multiple osteomyelitis infected with NTM [7]. Fewer patients of Asian origin have been reported with partial dominant IFNGR1 deficiency compared with those of Western countries [8]. The clinical phenotype of partial dominant IFNGR1 deficiency is milder than that of complete deficiency. In this type, BCG and NTM are the major pathogens. Complete IFN-γ receptor deficiency is associated with the early onset of severe disease caused by BCG or NTM, whereas the other genetic forms are associated with a milder course of mycobacterial infection [8].

Patients with partial IFGR1 deficiency usually respond well to antibiotic treatment, and for those who do not respond well, additional IFN-γ therapy has been shown to be effective [9]. There is no single standard regimen for the treatment of children with BCG osteomyelitis. *M. bovis* is resistant to pyrazinamides because of the expression of a pyrazinamidase. Case 1 was successfully treated with a long-term combination therapy of INH, RFP, and SM. However, in case 2, conventional therapy was inadequate to fight the infection. Additional administration of EB and relatively low dose IFN-γ was not able to control the intractable osteomyelitis. As NTM infection was also possible, high-dose EB, INH, and CAM were administered. The regimen was effective but temporary. Combination therapy, including LVFX and high-dose INF-γ, was the most successful strategy. Treatment with second-line antituberculous drugs, such as fluoroquinolone, and two first-line drugs (RFP and EB), may be more effective than RFP and EB alone against multidrug-resistant *M. bovis* [10]. LVFX plays an important role as a substitute agent for those patients who are intolerant of first-line antituberculous agents.

IFN-γ receptor deficiency is a rare disorder that should be considered when patients exhibit BCG lymphadenitis and disseminated osteomyelitis. Multifocal mycobacterial osteomyelitis without other organ involvement is only seen in dominant partial IFNGR1 deficiency [6, 8]. This type of immunodeficiency tends to exhibit recurrent mycobacterial infection and resistance to conventional antimycobacterial therapy. LVFX is likely an effective option for cases with the partial dominant type that are resistant.

References

1. Dupuis S, Döffinger R, Picard C, Fieschi C, Altare F, Jouanguy E, et al. Human interferon-γ-mediated immunity is a genetically controlled continuous trait that determines the outcome of mycobacterial invasion. Immunol Rev. 2000;178:129–37.
2. Filipe-Santos O, Bustamante J, Chapgier A, Vogt G, de Beaucoudrey L, Feinberg J, et al. Inborn errors of IL-12/23- and IFN-gamma-mediated immunity: molecular, cellular, and clinical features. Semin Immunol. 2006;18:347–61.
3. Sasaki Y, Nomura A, Kusuhara K, Takada H, Ahmed S, Obinata K, et al. Genetic basis of patients with Bacille Calmette–Guérin (BCG) osteomyelitis in Japan: identification of dominant partial interferon-γ receptor 1 deficiency as a predominant type. J Infect Dis. 2002;185:706–9.
4. Milstein JB, Gibson JJ. Quality control of BCG vaccine by WHO: a review of factors that may influence vaccine efficacy and safety. Bull WHO. 1990;68:93–108.
5. Toida I, Nakata S. Severe adverse reactions after vaccination with Japanese BCG vaccine: a review. Kekkaku. 2007;82:809–24 (in Japanese).
6. Hoshina T, Takada H, Sasaki-Mihara Y, Kusuhara K, Ohshima K, Okada S, Kobayashi M, Ohara O, Hara T. Clinical and host genetic characteristics of Mendelian susceptibility to mycobacterial disease in Japan. J Clin Immunol. 2011;31:309–14.
7. Lee W-I, Huang J-L, Lin T-Y, Hsueh C, Wong AM, Hsieh M-Y, et al. Chinese patients with defective IL-12/23-interferon-γ circuit in Taiwan: partial dominant interferon-γ receptor 1 mutation presenting as cutaneous granuloma and IL-12 receptor γ1 mutation as pneumatocele. J Clin Immunol. 2009;29:238–45.
8. Dorman SE, Picard C, Lammas D, Heyne K, van Dissel JT, Barreto R, et al. Clinical features of dominant and recessive interferon gamma receptor 1 deficiencies. Lancet. 2004;364:2113–21.
9. Remus N, Reichenbach J, Picard C, Rietschel C, Wood P, Lammas D, et al. Impaired interferon gamma-mediated immunity and susceptibility to mycobacterial infection in childhood. Pediatr Res. 2001;50:8–13.
10. Fennelly GJ. *Mycobacterium bovis* versus *Mycobacterium tuberculosis* as a cause of acute cervical lymphadenitis without pulmonary diseases. Pediatr Infect Dis J. 2004;23:590–1.

GENES, CHROMOSOMES & CANCER 52:274–286 (2013)

Meiosis Error and Subsequent Genetic and Epigenetic Alterations Invoke the Malignant Transformation of Germ Cell Tumor

Mizuho Ichikawa,[1,2] Yasuhito Arai,[3] Masayuki Haruta,[1] Shinsuke Furukawa,[1] Tadashi Ariga,[2] Tadashi Kajii,[4] and Yasuhiko Kaneko[1]*

[1]Research Institute for Clinical Oncology, Saitama Cancer Center, Ina, Saitama, Japan
[2]Department of Pediatrics, Hokkaido University Graduate School of Medicine, Sapporo, Hokkaido, Japan
[3]Division of Cancer Genomics, National Cancer Center Research Institute, Chuo-Ku, Tokyo, Japan
[4]Hachioji, Tokyo, Japan

Germ cell tumors (GCTs) are thought to arise from primordial germ cells (PGCs) that undergo epigenetic reprogramming. To explore the mechanisms of GCT formation, we analyzed single-nucleotide polymorphism array comparative genomic hybridization patterns and the methylation status of 15 tumor suppressor genes (TSGs) and differentially methylated regions (DMRs) of two imprinted genes, *H19* and *SNRPN*, in 28 children with GCTs. Three GCTs with 25–26 segmental uniparental disomies (UPDs), heterozygous centromeric regions, and a highly methylated *SNRPN* DMR may have occurred through meiosis I error. Three other GCTs with whole UPD and homozygous centromeric regions of all chromosomes may have occurred through endoreduplication of a haploid set in an ovum or testis. The other 22 GCTs had heterozygous centromeric regions of all chromosomes and no or a small number of segmental or whole UPDs and may have developed from premeiotic PGCs before imprint erasure or a reestablishment of imprinting. Gain and amplification of 3p24-p22 and 20q13-q13, and loss and UPD of 1p36-p35, 4q21-q21, 5q11-q13, and 6q26-qter were found in five or more tumors. 1p36-p35 loss was frequent, and found in 19 tumors; *RUNX3* residing at 1p36 was methylated in the promoter regions of 16 tumors. Two yolk sac tumors with many segmental UPDs or whole UPD of all chromosomes had gain of 20q13-q13 and loss of 1p36-p35, and seven or eight methylated TSGs. These genetic and epigenetic alterations may have caused malignant transformation because they were rarely found in teratomas with segmental or whole UPDs.

INTRODUCTION

Germ cell tumors (GCTs) are a heterogeneous group comprising both benign and malignant types. GCTs occur at an incidence of 2.4 per million children and represent ~ 1% of childhood cancers (Young et al., 1986). They are thought to arise from primordial germ cells (PGCs) that undergo epigenetic reprogramming (Oosterhuis and Looijenga, 2005).

In general, the formation of teratomas in ovaries appears to be a manifestation of defective meiosis. Using chromosomal heteromorphisms of the centromeric regions and distal polymorphic DNA markers, Surti et al. (1990) tried to clarify how ovarian teratomas form, and proposed five mechanisms based on when during meiosis the teratomas developed. However, they could not distinguish between meiosis I error (Type I) and fusion of two ova (Type V), or between meiosis II error (Type II) and endoreduplication (Type III), because of the limited numbers of heteromorphisms and DNA markers (Table 1; Fig. 1). Today, high-resolution single-nucleotide polymorphism (SNP) array-based analyses enable us to distinguish these types. However, there seem to be no studies of the mechanisms of germ cell tumorigenesis using SNP arrays.

Genomic imprinting is a phenomenon whereby paternal and maternal sets of chromosomes differ functionally in mammals due to parental-specific epigenetic modifications of the genome. PGCs undergo epigenetic reprogramming, that is, erasure of the somatic imprint in the genital ridge, and reestablishment of the sex-specific imprint at gametogenesis in the developing gonad. The *H19* gene is located at 11p15.5 and encodes a noncoding RNA and the gene *SNRPN* (small nuclear

Supported by: The third-term Comprehensive 10-Year Strategy for Cancer Control from the Ministry of Health, Labor, and Welfare, Japan.

*Correspondence to: Yasuhiko Kaneko, Research Institute for Clinical Oncology, Saitama Cancer Center, 818 Komuro, Ina, Saitama, 362-0806, Japan. E-mail: kaneko@cancer-c.pref.saitama.jp

Received 26 July 2012; Accepted 7 October 2012

DOI 10.1002/gcc.22027

Published online 8 December 2012 in Wiley Online Library (wileyonlinelibrary.com).

ribonucleoprotein associated polypeptide N) is located at 15q11-q13 and encodes SmN, a protein involved in spliceosomes (Gabory et al., 2006; Horsthemke and Buiting, 2006). It has been suggested that the pattern of *H19* and *SNRPN* methylation in GCTs can be used as a marker of gametic development of PGCs giving rise to tumors (Miura et al., 1999; Bussey et al., 2001; Schneider et al., 2001; Sievers et al., 2005). We previously analyzed the methylation status of *H19* and *SNRPN* differentially methylated regions (DMRs) in 45 GCTs, and found that 20 were in the abnormal epigenetic reprogramming pathways defined on the basis of the methylation status of the two DMRs and the anatomical site of tumors (Furukawa et al., 2009). The methylation pattern of the *H19* and *SNRPN* DMRs was mostly physiological in teratomas and varied in yolk sac tumors. Furthermore, we evaluated the methylation status of the promoter region of 15 tumor suppressor genes (TSGs), and found that yolk sac tumors had a higher number of methylated TSGs than teratomas or other childhood tumors.

Using array comparative genomic hybridization, several groups have found that childhood GCTs have characteristic patterns of genomic imbalance, including 1p−, 1q+, 6q−, and 20q+ (Mostert et al., 2000; van Echten et al., 2002; Schneider et al., 2006). Particular histological subtypes of GCT have been correlated with similar patterns of genomic imbalance irrespective of the site at which they occur (Riopel et al., 1998; Perlman et al., 2000; Rickert et al., 2000; Schneider et al., 2002; Palmer et al., 2007); a finding

TABLE 1. Mechanisms of Origin of Ovarian Teratomas (Surti et al., 1990)

		Teratoma genotype at[a]	
Type	Mechanism	Centromere	Distal marker
I	Meiosis I error	+	+, −
II	Meiosis II error	−	+, −
III	Endoreduplication	−	−
IV	No meiosis	+	+
V	Fusion of two ova	+, −	+, −

[a]+ = heterozygous; − = homozygous.

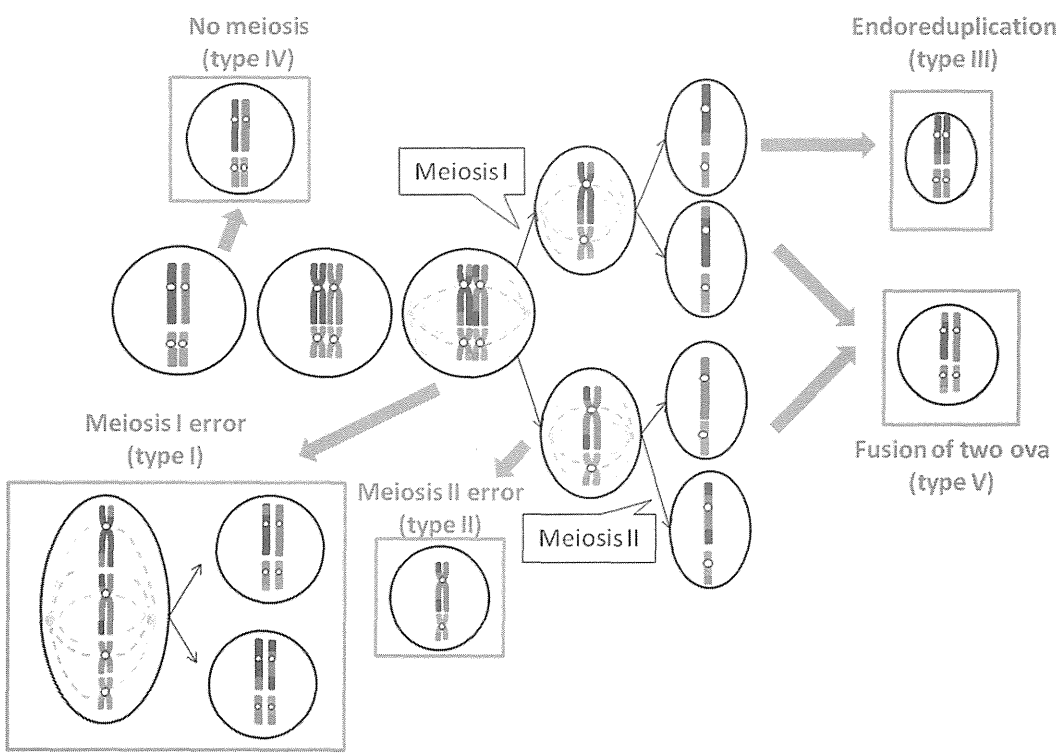

Figure 1. The scheme of meiosis and germ cell tumorigenesis. The exact nature of the meiotic error can be discerned in most cases with the use of SNP arrays. Meiosis I error (Type I) would result in heterozygosity for all centromeric markers for which the host was heterozygous, whereas distal markers could be heterozygous by the occurrence of crossing-over. Meiosis II error (Type II) would result in homozygosity near the centromeric regions, and distal markers could be heterozygous. Endoreduplication (Type III) would lead to homozygosity in all centromeric and distal markers. Total lack of meiosis of a primordial germ cell (Type IV), followed by mitotic division, would produce GCTs in which all centromeric and distal markers would be identical to the host. Fusion of two ova (Type V) would, on average, results in an equal number of heterozygous and homozygous centromeric and distal markers. [Color figure can be viewed in the online issue, which is available at wileyonlinelibrary.com.]

consistent with the hypothesis that they arise from the same progenitor cell. To explore the mechanisms of GCT formation, we analyzed genetic and epigenetic alterations in GCTs with a high-resolution SNP array and the methylation status of TSGs and *H19* and *SNRPN* DMRs.

MATERIALS AND METHODS

Patients and Samples

Tumor tissues were obtained from 28 children with GCT. There were 13 males and 15 females, ranging in age from 1 month to 14 years with a median age of 3 years (Table 2). In all tumors, the diagnosis of GCT was made by pathologists at each institution according to the classification proposed by Woodward et al. (2004) and/or the Japanese Pathological Society (1999). The pathologists verified that each sample for molecular genetic analysis contained 70% or more tumor cells. Tumor tissues, which were obtained at Saitama Cancer Center or sent from other hospitals, were immediately frozen after resection or on arrival at the center. The study design was approved by the ethics committee of Saitama Cancer Center. The tumors were histologically classified into 24 cases of yolk sac tumor, 1 case of immature teratoma, and 3 cases of mature teratoma.

Representative histology was used for one yolk sac tumor (Case 10) and one mature teratoma (Case 4) that showed more than one histological criterion. Twenty-two tumors originated from the gonad (ovary, 12; testis, 10), and six from extragonadal sites (mediastinum, 2; the sacrococcygeal region, 2; retroperitoneum, 1; and stomach, 1). Data on outcome were available for all 28 patients. One (No. 16) died of the disease, whereas the other patients were alive at the last follow-up.

Copy Number and Loss of Heterozygosity (LOH) Analysis Using SNP Arrays

High-resolution Affymetrix Mapping 250K-Nsp arrays (Affymetrix, Santa Clara, CA) were used to analyze the chromosomal copy number and LOH status in the 28 tumors as described previously (Haruta et al., 2008). Uniparental disomy (UPD) was defined as a region of copy number-neutral LOH spanning over 3 Mb. Copy numbers and LOH were calculated using CNAG and AsCNAR programs with paired (7 cases) or anonymous (21 cases) references as controls (Nannya et al., 2005; Yamamoto et al., 2007).

Bisulfite Treatment and Combined Bisulfate Restriction Assay (COBRA) of the CTCF6-Binding Site at *H19* DMR and the 5′-Untranslated Region of *SNRPN* DMR

Genomic DNA from tumor samples was treated with sodium bisulfite and COBRA was performed to determine the methylation status of the CCCTC-binding factor-binding site 6 (CTCF6)-binding site at *H19* DMR, as described previously (Watanabe et al., 2007). In addition, we also evaluated the methylation status of the 5′-untranslated region of the *SNRPN* DMR (Kobayashi et al., 2007). *Mlu*I and *Cfo*I were used as restriction enzymes to evaluate the methylation status of the *H19* and *SNRPN* DMRs, respectively. The intensity of methylated and unmethylated bands was examined by a fluoroimage analyzer, FLA-3000G (Fujifilm, Tokyo, Japan). Two methylated bands, 197 and 82 bp, represented the *H19* DMR, but the smaller band was too faint to be evaluated. Likewise, two methylated bands, 175 and 65 bp, represented the *SNRPN* DMR, but only the larger band was evaluated. The experiments were performed three times, and the mean value of the DNA methylation percentages was calculated.

Methylation-Specific PCR (MSP) Analysis of Various TSGs

The methylation status of the promoter region in 15 TSGs was analyzed by MSP, as previously reported (Lind et al., 2006; Honda et al., 2008). The genes examined were *RASSF1A*, *HOXA9*, *RUNX3*, *CASP8*, *SCGB3A1*, *SFRP2*, *DCR2*, *RASSF5*, *RASSF2A*, *BLU*, *SFRP5*, *HOXB5*, *p16INK4A*, *p14ARF*, and *RIZ1*. The primer sequences and their location in the original genomic sequences were also shown in the reports cited above. CpG genome™ Universal Methylated DNA (Chemicon International, Temecula, CA) and normal lymphocyte DNA were used as controls for completely methylated/ unmethylated templates, respectively. PCR products were run on 2% agarose gels and visualized after staining with ethidium bromide.

Mutation Analysis of the *RUNX3* Gene

To detect point mutations and deletions of the *RUNX3* gene, we performed direct sequencing of the Runt domain, which is highly conserved and

TABLE 2. Age, Histology, SNP Profiles, Number of Methylated Tumor Suppressor Genes, and Methylation Status of *H19* and *SNRPN* DMRs in 28 GCTs

	Age	Sex	Site	Histology	Chromosomal gain and loss (total number of aberrations)	UPD (numbers)	Methylated TSGs	*H19*/ *SNRPN*
1	9 year	F	Ovary	MT	Normal (0)	Segmental (26)	1	UU/MM
2	4 year	F	Ovary	IT	+14 (1)	Segmental (26)	1	UU/MM
3	11 year	F	Ovary	YST	Xq−, 1p−, 1q+, 4p−, 4q−, 20q+, 22q+ (7)	Segmental (25)	7	UU/MM
4	6 year	F	Ovary	MT (YST)	Normal (0)	Whole (23)	1	UU/MM
5	1 year	M	Testis	YST	Normal (0)	Whole (22)	3	MU/UU
6	9 year	F	Ovary	YST	1p−, 1p+, 1q+, 3p+, 4q−, 6q−, 10q+, 20p−, 20q+, 22q−, 22q+ (11)	Whole (23)	8	UU/UM
7	5 month	F	Mediastinum	MT	1p−(1)	(0)	0	MU/UM
8	9 year	F	Ovary	YST	12p+, 20q+, +21 (3)	Whole (1)	5	UU/UU
9	1 year	M	Retroperito	YST	Normal (0)	(0)	1	MM/UM
10	6 year	F	Ovary	YST (MT)	1p+, 1q+, 2p+, 4q−, 6q−, 10p−, 20q+ (7)	(0)	9	MM/UM
11	14 year	F	Ovary	YST	1p−, 2q−, 4q−, 5p−, 5q−, −6, 9q+, 11p−, 11q−, 12p+, −13, −14, −16, 17p−, 17q+, −18, −19, +21 (18)	Whole (2)	6	UU/UU
12	2 year	M	Testis	YST	1p−, 2q−, 3p+, 3q+, −4, 6q−, 8q−, 9q+, 9q−, 10q−, 12q+, 13q+, 17q−, +20, 21q−, +22 (16)	Whole(1), Segmental (3)	5	UU/UU
13	11 year	F	Ovary	YST	6p+, 6q−, 7q+, 16q−, 20q+ (5)	Segmental (1)	3	MU/UM
14	1 year	F	Sacrococcy	YST	1p−, 3p+, 4q−, 5q−, 6q−, 10q−, 13q+, 20p−, 20q+, 21q+ (10)	Segmental (1)	7	MM/UM
15	10 year	M	Mediastinum	YST	1q−, 1q+, 2p+, 2q−, 4q−, 5q−, 6q−, 7p+, 8p+, 10p−, 20p−, 20q+, 22q−(13)	Segmental (1)	7	UU/UU
16	10 month	F	Sacrococcy	YST	1p−, 1q+, 2p+, 2q+, 4p−, 4q−, −5, −6, 9q−, +12, +14, 20q+, −21 (13)	(0)	8	MU/UM
17	14 year	F	Ovary	YST	1p−, 4q+ (2)	(0)	4	MU/UM
18	1 year	M	Testis	YST	1p−, −4, 12q+, −16, 20q+, +21 (6)	(0)	6	MU/UU
19	2 year	M	Testis	YST	1p−, 3p+, 3p−, 3q−, −4, 9p−, 9q−, 15q+ (8)	(0)	8	MU/UU
20	1 year	M	Testis	YST	1p−, 4q−, 6q−, 11q+, 11q−, 16p−, 16q+, 16q−(8)	(0)	3	UU/UU
21	13 year	F	Ovary	YST	−6 (1)	Segmental (4)	8	UU/UU
22	9 year	F	Ovary	YST	1p−, 9q−, 20q+ (3)	Segmental (1)	5	MU/UM
23	6 month	M	Testis	YST	1p−, 3p+, 3q−, 6p+, 6q−, −15, 17p−, 17q−, 20p−, 20q+, (10)	(0)	7	MU/UU
24	1 month	M	Testis	YST	1p−, 6q−, +10, 11p−, 17q−, 19p+, 20q+ (7)	(0)	6	MU/UM
25	11 month	M	Testis	YST	1p−, 1q+, 2p+, 6q−, 9p−, 9q−, 12p+, −13, −14, −15, 16p−, 17q−, 20p−, 20q+ (14)	(0)	6	MU/UU
26	1 year	M	Testis	YST	1p−, 1q+, −4, 5q−, 6q−, −8, 9p−, 11q+, 13q−, 20q+ (10)	Segmental (1)	2	UU/UU
27	8 year	M	Testis	YST	3p+, 4q+, 6q−, 7q+, 8p+, −10, −11, 12p+, −13, 16q−, −18, 19q− (12)	(0)	0	UU/UU
28	2 year	M	Stomach	YST	1p−, 1q+, −4, 6q−, 7p+, −15, 18q−, 20p−, 20q+ (9)	Segmental (1)	6	UU/UM

F, female; M, male; Retroperito, retroperitoneum; Sacrococcy, sacrococcygeal region; YST, yolk sac tumor; MT, mature teratoma; IT, immature teratoma; UPD, uniparental disomy; U, unmethylated allele; M, methylated allele; TSG, tumor suppressor gene; UU/MM, see legend for Figure 2.

responsible for DNA-binding and protein-protein interaction. Genomic DNA from two tumor samples with a *RUNX3* deletion and unmethylated *RUNX3* was amplified using four sets of primers, RUNX3 ex2bF, 5′-CCGTAGACCCAAGCAC CAG -3′, and RUNX3 ex2bR, 5′-CACTGCTCCC GAGGCTCT-3′, and RUNX3 ex3F 5′- TTCC CTGGTCACCCTCTTC-3′, and RUNX3 ex3R, 5′-TAAGGCCCCTCTTTCAACCT-3′, and RUNX3 ex4F, 5′-AGGTGGGAGAGCAGGGTATT-3′, and RUNX3 ex4R, 5′-TAAGCCCAGAGGGTT TAGGG-3′, and RUNX3 ex5F, 5′-ACTGAG ACTCTGGGGAAGCA-3′, and RUNX3 ex5R, 5′-GTACCTTGGATTGGGGTCTG-3′, respectively. The PCR products were directly sequenced with a BigDye (R) Terminator Cycle sequencing kit on an automated ABI PRISM (R) 310 sequencer (Applied Biosystems, Foster City, CA).

Statistical analysis

We assessed the association between the number of chromosome aberrations and that of methylated TSGs by determining the Spearman rank correlation coefficient and associated *P*-value.

RESULTS

Methylation Analysis of *H19* and *SNRPN* DMRs

We examined the methylation status of *H19* and *SNRPN* DMRs using COBRA. We chose a cut-off value of <33.3% methylation, between 33.3% and 66.6% methylation, and >66.6% methylation as definitions of hypomethylated, somatically methylated, and hypermethylated states, respectively (Sievers et al., 2005; Furukawa et al., 2009). Among the 28 tumors, the *H19* DMR was hypomethylated in 14 tumors, somatically methylated in 11 tumors, and hypermethylated in 3 tumors, and the *SNRPN* DMR was hypomethylated in 13 tumors, somatically methylated in 11 tumors, and hypermethylated in 4 tumors (Table 2; Fig. 2).

Chromosomal Aberrations and UPD Regions Detected with SNP Arrays

In the SNP array analyses, only one showed a normal chromosome pattern (Table 2). Three tumors (Cases 1, 2, and 3) showed 25 to 26 segmental UPDs, and one of the three had chromosome gains and losses additional to the segmental UPDs (Figs. 3A and 3B). Three other tumors (Cases 4, 5, and 6) showed whole chromosomal UPD in all chromosomes, and one of the three also had gains and losses in addition to the whole UPDs (Figs. 4A and 4B).

Of the 28 tumors, 24 showed chromosomal gains or losses, and 4 showed no chromosomal aberrations; three of these four had many segmental UPDs or whole UPD in all chromosomes (Table 2). Chromosomal gains of 3p24-p22 and 20q13-q13 and losses and UPDs of 1p36-p35, 4q21-q21, 5q11-q13, and 6q26-qter were found in five or more tumors (Fig. 5). The shortest overlapping regions for gain and amplification of 3p24-p22 and 20q13-q13, and for loss and UPD of 1p36-p35, 4q21-q21, 5q11-q13, and 6q26-qter are summarized in Table 3.

MSP Analysis of Various TSGs in GCTs and Mutation Analysis of the *RUNX3* Gene

We examined the methylation status of 15 TSGs in the 28 GCT samples by MSP, and found hypermethylation of *RASSF1A* in 21 (75.0%), *HOXA9* in 21 (75.0%), *RUNX3* in 21 (75.0), *CASP8* in 13 (46.4%), *SCGB3A1* in 15 (53.6%), *SFRP2* in 13 (46.4%), *DCR2* in 14 (50.0%), *RASSF5* in seven (25.0%), *RASSF2A* in five (20.8%), examined in 24 samples, *BLU* in three (10.7%), *SFRP5* in one (3.6%), *HOXB5* in one (3.6%), and *SFRP1* in one (3.6%; Table 4). No tumors showed hypermethylation of *p16INK4A*, *p14ARF*, or *RIZ1*.

Notably, the present SNP array study showed loss of 1p36-p35 in 19 of the 28 tumors. *RUNX3* is located at 1p36.11 and its promoter region was methylated in 16 of the 19 tumors (Table 4). Genomic DNA was available in 2 of 3 tumors with 1p36 loss and unmethylated *RUNX3*. No point mutation was detected in the Runt domain of these two tumors by sequencing (Cases 26 and 27; Table 4).

The Spearman correlation coefficient analysis showed that the numbers of chromosome aberrations correlated with those of methylated TSGs in the six tumors with many segmental or whole UPDs ($rS = 0.946$, $P = 0.004$), and in all 28 tumors ($rS = 0.43$, $P = 0.021$; Tables 2 and 4).

Tumor Origin Estimated from COBRA and SNP Array Patterns

Multiple segmental UPD regions were observed in many chromosomes, and SNP patterns of the centromeric regions were heterozygous in three tumors (Cases 1, 2, and 3; Figs. 3A

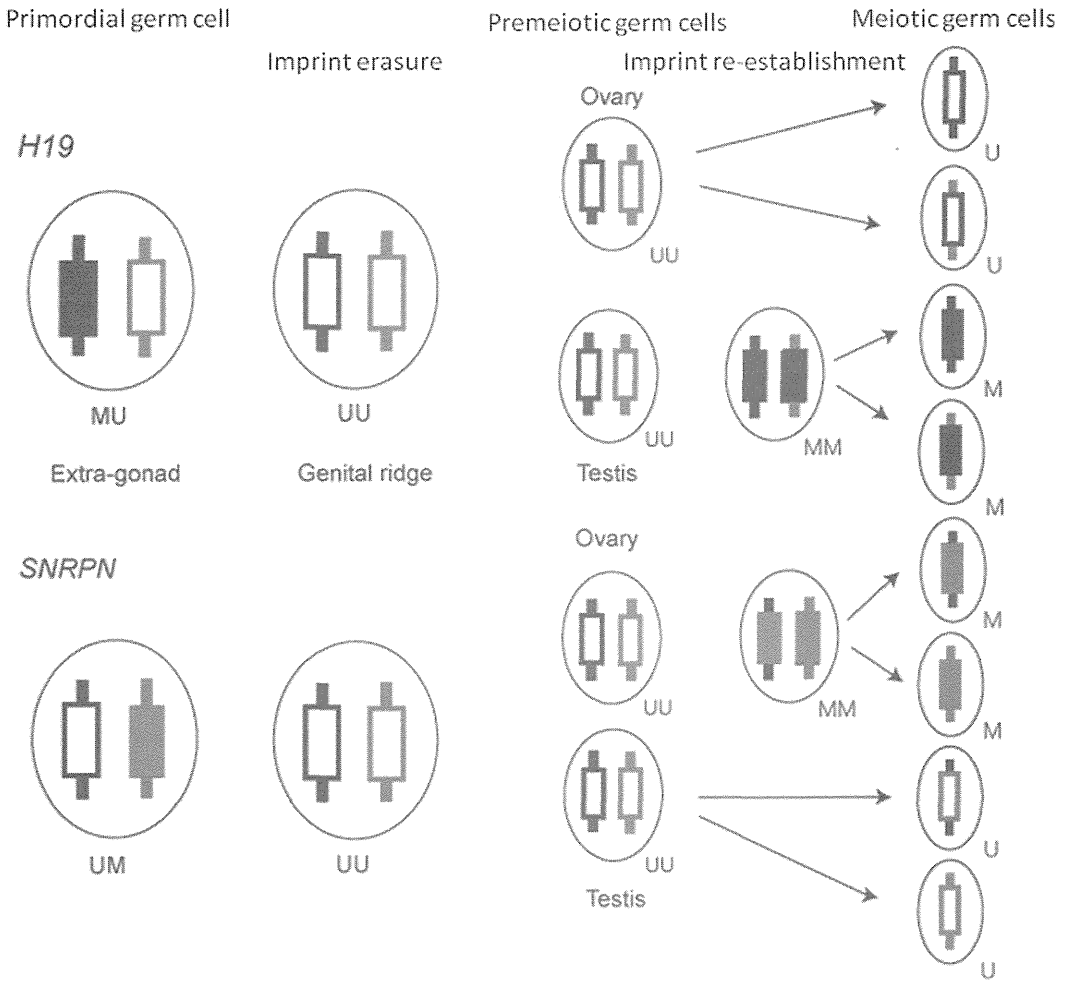

Figure 2. Model of *H19* and *SNRPN* imprint resetting in the human germline. Primordial germ cells (PGCs) before entering the genital ridge retain a somatic methylation pattern showing the paternal imprint in the *H19* differential methylated region (DMR) and maternal imprint in the *SNRPN* DMR (*H19* DMR/*SNRPN* DMR is shown as MU/UM). When PGCs have entered the genital ridge, both homologs are unmethylated and the imprint is erased (UU/UU). The imprint is reestablished when both homologs of the *H19* DMR in male PGCs are methylated (MM) at the premeiotic stage in the testis and both homologs of the *SNRPN* DMR in female PGCs are methylated (MM) at meiosis in the ovary. M, methylated DMR; U, unmethylated DMR. [Color figure can be viewed in the online issue, which is available at wileyonlinelibrary.com.]

and 3B). In these ovarian GCTs, the *SNRPN* DMR was highly methylated, indicating that the tumors were originated from PGCs after the reestablishment of imprinting. Meiosis I error might be the mechanism of tumorigenesis of these three tumors because of heterozygosity in all centromeric regions and multiple segmental UPDs possibly caused by crossing-over of meiotic homologous chromosomes.

Whole chromosomal UPD was observed in all chromosomes, and SNP patterns of all centromeric regions were homozygous in another three tumors (Cases 4, 5, and 6; Figs. 4A and 4B). The *SNRPN* DMR was hypermethylated in an ovarian teratoma, and methylated in an ovarian yolk sac tumor, and *H19* DMR was methylated in a testicular yolk sac tumor, indicating that the tumors originated from PGCs that were undergoing epigenetic reprogramming. These findings indicate endoreduplication to be the mechanism of tumorigenesis of these tumors.

Chromosomal gains and losses in addition to the segmental or whole UPDs and many methylated TSGs were observed in two ovarian yolk sac tumors (Tables 2 and 4; Figs. 3B and 4B). Chromosomal gains and losses, and methylated TSGs were also found in other GCTs without many segmental or whole UPDs (Cases 7–28). These copy number and epigenetic alterations, considered to arise after the occurrence of UPD, are rarely found in mature or immature teratomas (Cases 1, 2, and 4) suggesting the alterations to

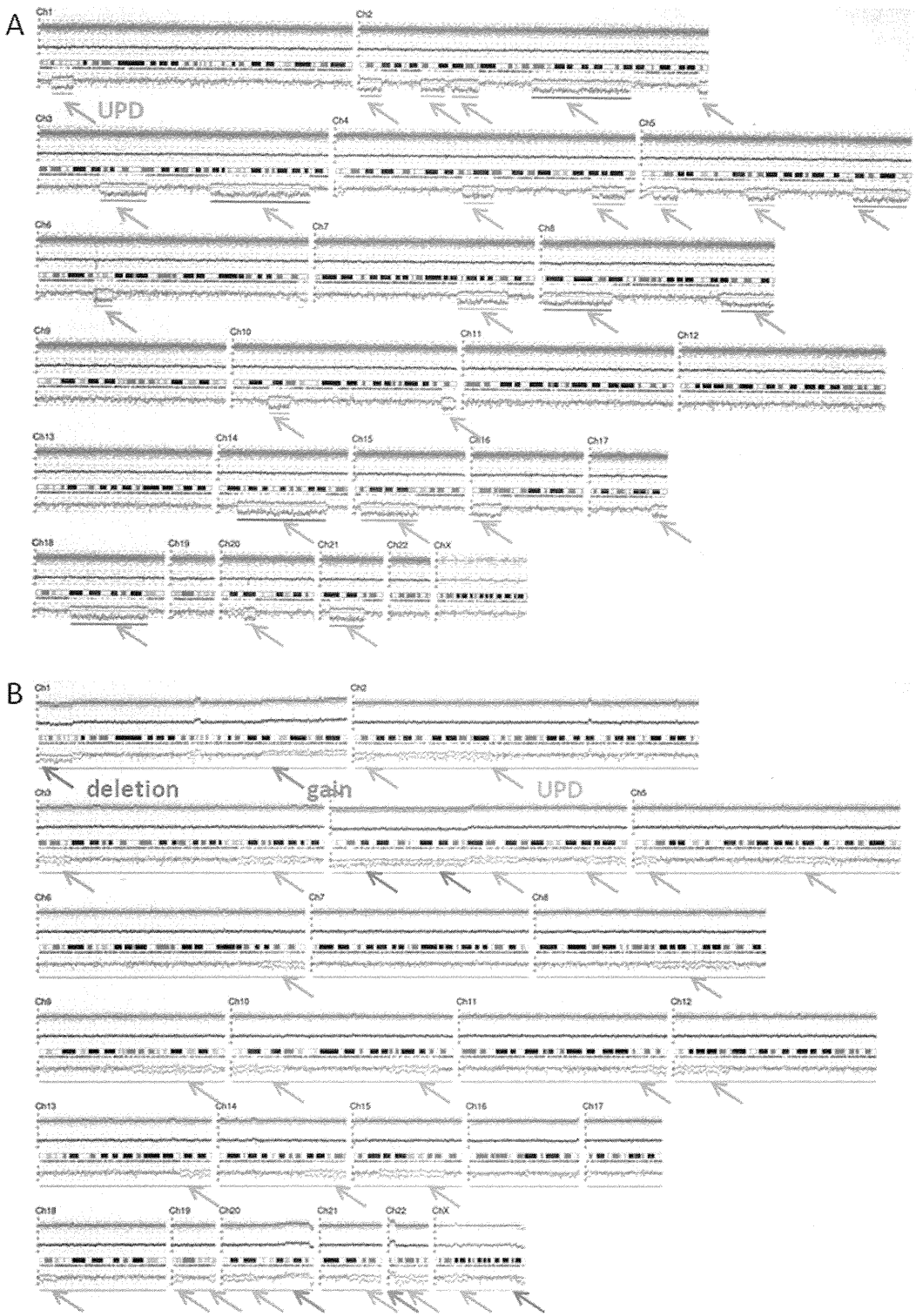

Figure 3. SNP array patterns of two tumors (A, Case 1 and B, Case 3). The blue line indicates the log2-ratio of the total copy number of each chromosomal region. Red and green lines indicate the log2-ratio of the allele-specific copy number. (A) Multiple segmental UPDs (green arrows) were observed in the distal regions of many chromosomes. SNP patterns of centromeric regions were heterozygous, and those of distal regions were heterozygous or homozygous. (B) The tumor (Case 3) showed chromosomal gains of 1q, 20q, and 22q (red arrows), and losses of 1p−, 4p−, 4q−, and Xq− (blue arrows), in addition to many segmental UPDs. [Color figure can be viewed in the online issue, which is available at wileyonlinelibrary.com.]

Figure 4. SNP array patterns of two tumors (A, Case 4 and B, Case 6). The blue line indicates the log2-ratio of the total copy number of each chromosomal region. Red and green lines indicate the log2-ratio of the allele-specific copy number. A: Whole UPD in all chromosomes was observed. SNP patterns show homozygosity in all centromeric and distal regions. B: The tumor (Case 6) showed chromosomal gains of 1p, 1q, 3p, 10q, 20q, and 22q (red arrows), and losses of 1p, 4q, 6q, 20p, and 22q (blue arrows), in addition to whole UPD in all chromosomes. [Color figure can be viewed in the online issue, which is available at wileyonlinelibrary.com.]

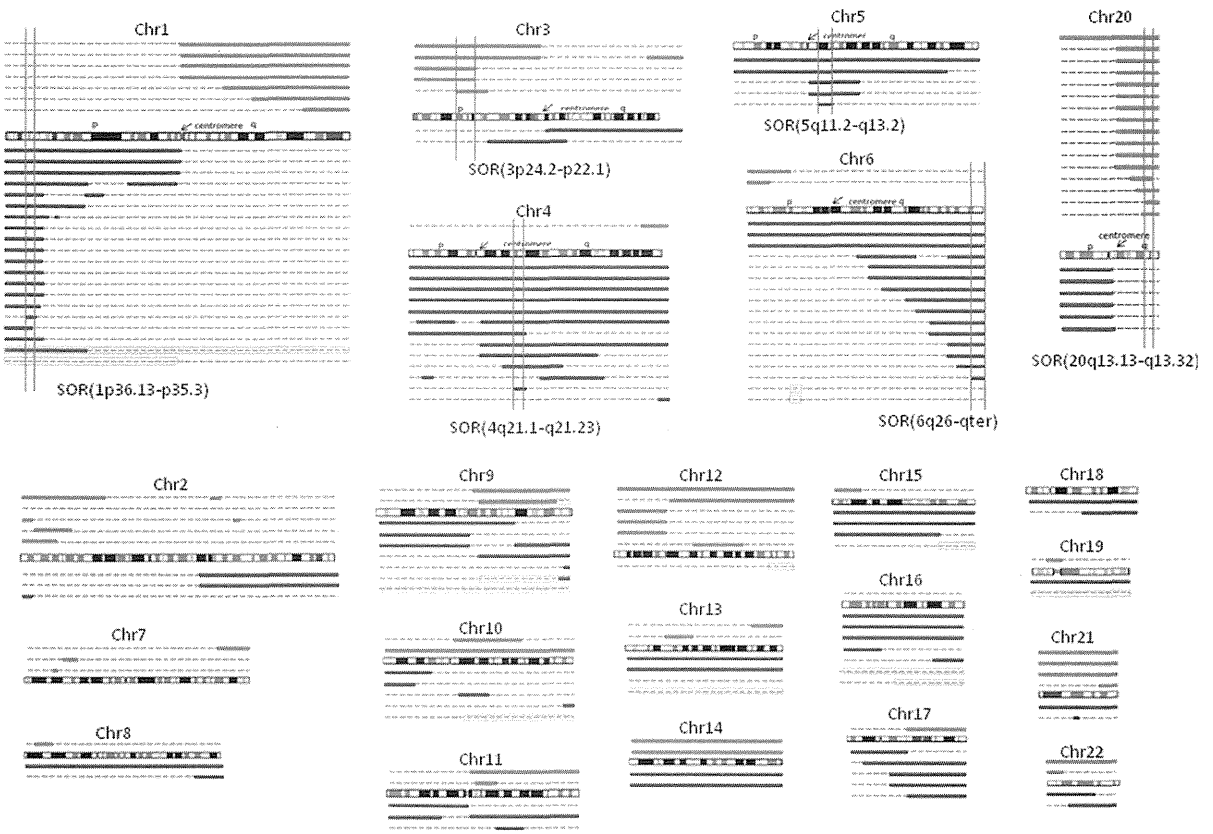

Figure 5. Summary of chromosomal alterations detected by SNP array analyses of 28 GCTs. Hemizygous deletions (blue lines) are shown under chromosomes, gains (red lines) are shown above chromosomes, and UPDs (green boxes) are shown mainly under chromosomes. Dotted lines indicate normal chromosome copies. Segmental and whole UPDs in six tumors (Cases 1–6) were excluded. Chr 1, chromosome 1; SOR, shortest overlapping region. [Color figure can be viewed in the online issue, which is available at wileyonlinelibrary.com.]

be involved in malignant transformation. Given the methylation patterns of *H19/SNRPN* DMRs, 22 tumors (Cases 7–28) are thought to be derived from premeiotic PGCs before the imprint erasure or before the reestablishment of imprinting.

DISCUSSION

In this study, we have for the first time found evidence that a benign teratoma could evolve to a malignant tumor such as a yolk sac tumor. SNP array and COBRA analyses allowed us to identify the mechanism of childhood teratoma and yolk sac tumor formation. Previous studies using chromosomal heteromorphisms and polymorphic DNA markers indicated that ovarian tetratoma could be classified into five subtypes (Table 1; Fig. 1) (Surti et al., 1990); Type I (meiosis I error) showing heterozygous centromeric regions, and heterozygosity and homozygosity in distal regions depending on the occurrence of crossing-over, Type II (meiosis II error) showing homozygous centromeric regions and heterozygosity and homozygosity in distal regions depending on the occurrence of crossing-over, Type III (endoreduplication) showing homozygosity in centromeric and distal regions in all chromosomes, Type IV (no meiosis) showing heterozygosity in centromeric and distal regions, and Type V (fusion of two ova) showing a combination of homozygosity and heterozygosity in centromeric and distal regions.

The present SNP array analysis revealed a specific allelic status of Types I and III, that is, segmental UPDs in various chromosomes and whole UPD in all chromosomes, respectively, which were mostly found in teratomas and a small number of yolk sac tumors. Segmental and whole UPDs were also found in Type IV tumors, consisting of the great majority of yolk sac tumors; however, the numbers of segmental UPDs and whole UPDs were less than five in this type. Thus, the three types of tumors were easily distinguishable. Previous studies using classical methods could not distinguish between Types I and V, or between Types II and III because of the limited numbers of